High-resolution measurement of Beutler-Fano profiles for autoionizing Rydberg series of Xe

Kengo Maeda
Kumamoto University, Faculty of Education, Kumamoto 860, Japan

Kiyoshi Ueda and Takeshi Namioka
Tohoku University, Research Institute for Scientific Measurements, Sendai 980, Japan

Kenji Ito
National Laboratory for High Energy Physics, Photon Factory, Tsukuba 305, Japan

(Received 18 March 1991; revised manuscript received 30 July 1991)

Photoabsorption cross sections for the ns' and nd' autoionizing Rydberg series of Xe have been measured with a resolution of 7.4 mÅ using a high-resolution spectrometer and synchrotron radiation. The cross sections are parametrized with the aid of a line-shape formula that is based on the multichannel-quantum-defect theory and has a form analogous to Fano's resonance formula and are compared in detail with theoretical predictions available in the literature.

PACS number(s): 32.80.Dz, 32.70.Jz

I. INTRODUCTION

Dipole-allowed single-electron excitation from the $mp^6\,{}^1S_0$ ground state of rare gases ($m=3$, 4, and 5 on Ar, Kr, and Xe, respectively) leads to the $J=1$ odd-parity levels, which belong to five Rydberg series $mp^5({}^2P_{3/2})ns[3/2]^o_1$, $mp^5({}^2P_{3/2})nd[1/2]^o_1$, $mp^5({}^2P_{3/2})nd[3/2]^o_1$, $mp^5({}^2P_{1/2})ns'[1/2]^o_1$, and $mp^5({}^2P_{1/2})nd'[3/2]^o_1$. The former three series built on the $mp^5\,{}^2P_{3/2}$ ion core converge to the first limit $I_{3/2}$ and the latter two series ns' and nd' built on $mp^5\,{}^2P_{1/2}$ converge to the second limit $I_{1/2}$. Between $I_{3/2}$ and $I_{1/2}$, the ns' and nd' series are subject to autoionization. Photoabsorption spectra for these autoionization resonances of rare gases were first observed by Beutler [1] and theoretically analyzed by Fano [2]. Thus characteristic line shapes of the autoionization resonances are often called Beutler-Fano profile.

Since the pioneering work by Beutler [1], much work has been devoted to the study of these autoionization resonances of rare gases. In the case of Xe which we are concerned with here, peak positions of the ns' and nd' resonances were measured with high accuracy (<5 mÅ) by Yoshino and Freeman [3] using a high-resolution vuv spectrograph, Bonin, McIlrath, and Yoshino [4] using a tunable vuv laser, and Wang and Knight [5] by means of two-photon laser spectroscopy. Bonin, McIlrath, and Yoshino [4] measured also a line shape of the $11s'$ resonance with a resolution of 2 mÅ [full width at half maximum (FWHM)]. Absolute photoabsorption cross sections in the autoionization region were measured by Huffmann, Tanaka, and Larrabee [6], Metzger and Cook [7], and Matsunaga, Jackson, and Watanabe [8] with moderate resolutions (200–500 mÅ) and relative cross sections were measured by Eland [9] with a resolution of 70 mÅ. Very recently, Wu *et al.* [10] measured relative cross sections and angular distribution parameters β across $8s'$ and $6d'$ resonances with a resolution of 26 mÅ by means of synchrotron-based photoelectron spectroscopy.

Recent theoretical investigations of the Beutler-Fano autoionization resonances of rare gases were based on the multichannel-quantum-defect theory (MQDT) [11,12]. Geiger [13] calculated Beutler-Fano profiles of autoionization resonances for Kr and Xe using MQDT parameters obtained by semiempirical MQDT analysis [12] of discrete energy levels and oscillator strengths. Johnson *et al.* [14] studied autoionization resonances of rare gases using relativistic MQDT: they obtained MQDT parameters from an *ab initio* relativistic-random-phase-approximation (RRPA) calculation. Connerade [15] analyzed the Xe autoionization resonances observed at a moderate resolution using the MQDT formulation of Dubau and Seaton [16].

In the present work, we have measured the absolute photoabsorption cross sections for Xe in the whole autoionization region with a resolution of 7.4 mÅ and then parametrized the cross sections with the aid of a line-shape formula [17] which is based on MQDT [11] and has a form analogous to Fano's resonance formula [18]. We compare the obtained Beutler-Fano line-shape parameters with the theoretical predictions [13,14], illustrating that the high-resolution line-shape measurement provides a sensitive test for the MQDT parameters.

II. EXPERIMENT

The apparatus and procedure are almost the same as those in our previous measurement for Kr [19,20] and thus a brief account is given here. The measurement was carried out at the Photon Factory by using the high-resolution facility [21] which consists of a 6.65-m off-plane Eagle-type monochromator-spectrograph (6VOPE) and a zero-dispersion tandem concave grating predisperser. The main spectrometer tank served as an absorption cell and the Xe pressures were 4.7×10^{-5}–1.9×10^{-4} Torr. The 6.65-m grating of the 6VOPE, having 1200 grooves/mm and blazed at 5500 Å, was used in the sixth spectral order. The 6VOPE was operated in the focal-plane-scanning mode, in which an exit slit and photon detector move along the focal plane while the predisperser system and the main grating remain fixed. The entrance and exit slits widths were 10 μm, resulting in a measured Gaussian instrumental profile of approximately 7.4 mÅ FWHM.

III. RESULTS

In Fig. 1, a part of the measured absolute photoabsorption cross sections σ is plotted as a function of $\nu_{1/2}=[R/(I_{1/2}-E)]^{1/2}$, where E and R are the excitation energy and the Rydberg constant, respectively. In the absence of the s-d interaction, which we assume to be the case, the Beutler-Fano profile in Fig. 1 can be described by the following expression [17], which has a form analogous to Fano's resonance formula [18] and is based on the Seaton's MQDT [11]:

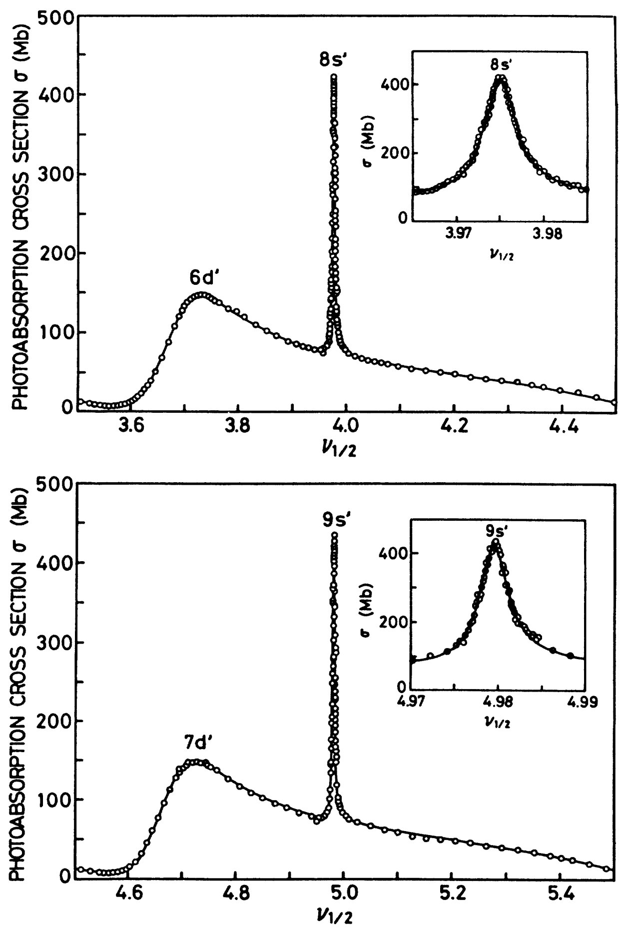

FIG. 1. Photoabsorption cross sections σ are plotted as a function of $\nu_{1/2}$. ○, the present measurement; solid lines, the results of the curve fit with Eqs. (1) and (2).

$$\sigma=\sigma_{as}\frac{(\varepsilon_s+q_s)^2}{1+\varepsilon_s^2}+\sigma_{ad}\frac{(\varepsilon_d+q_d)^2}{1+\varepsilon_d^2}+\sigma_b\ , \tag{1}$$

where ε_l is a periodic energy scale as given by

$$\varepsilon_l=\frac{\tan[\pi(\nu_{1/2}+\mu_l)]}{W_l}\ , \tag{2}$$

for $l=s$ and d. In Eq. (1), q_s and q_d are Fano's profile indices for the s' and d' resonances, respectively, σ_{as} and σ_{ad} represent the portions of the cross section describing transitions to open channels that interact with the closed s and d channels, respectively, and σ_b is a nonresonant portion of the cross section. In Eq. (2), μ_l's and W_l's are the quantum defects and the width parameters, respectively. The present line-shape parameters μ_l, W_l, q_l, σ_{al}, and σ_b were related to the MQDT parameters in our previous paper [17]. The width parameter W_l is related to the resonance width Γ_{nl} through the relation [17]

$$\frac{\Gamma_{nl}}{2}=\frac{2RW_l}{\pi(n-\mu_l)^3}\ . \tag{3}$$

The nine parameters μ_l, W_l, q_l, σ_{al}, and σ_b can be obtained for each resonance pair by means of a least-squares curve-fitting method. The solid curves drawn in Fig. 1 are an example of the results of the curve fitting. Every fitted curve passes through the experimental data points, suggesting the adequacy of Eqs. (1) and (2) as a parametric expression for the Beutler-Fano profile of the Xe ns' and nd' autoionizing Rydberg series. The resultant line-shape parameters of the ns' and nd' resonances are plotted with open circles (○) in Fig. 2 as a function of excitation photon energy (in units of eV).

We have investigated the effect of finite instrumental width in the following manner. We first reproduce the absorption data $I_a(\lambda)$ from the above-obtained absorption cross section $\sigma_{\rm obs}$:

$$I_a(\lambda)=\exp[-\sigma_{\rm obs}(\lambda)Nl]\ , \tag{4}$$

where Nl is a column density of the Xe gas. Note that $I_a(\lambda)$ given by Eq. (4) does not represent the observed absorption data because $\sigma_{\rm obs}(\lambda)$ was obtained by correcting the absorption data for scattered light and slow variation in Nl during the measurement [20]. The $I_a(\lambda)$ data are then fitted with

$$I_{a'}(\lambda)\equiv\int_{-\Delta\lambda}^{+\Delta\lambda}\exp[-\sigma_{th}(\lambda+\delta\lambda)Nl]F(\delta\lambda)d\delta\lambda\ , \tag{5}$$

where $\sigma_{th}(\lambda)$ is expressed by Eq. (1) and the response of the instrument to monochromatic radiation, $F(\delta\lambda)$, is assumed to have a Gaussian profile with a FWHM of 7.4 mÅ. The range of integration, $2\Delta\lambda$, is taken to be 33 mÅ. The line-shape parameters thus obtained for certain members are also shown in Fig. 2 by solid circles (●).

In Fig. 2(c), we compare the width parameters W_s corrected for the instrumental effect (●) with the original ones which are not corrected for the instrumental effect (○). The original W_s increases rapidly with an increase in energy for $n>11$, whereas the corrected W_s decreases very slowly with an increase in energy. The abrupt in-

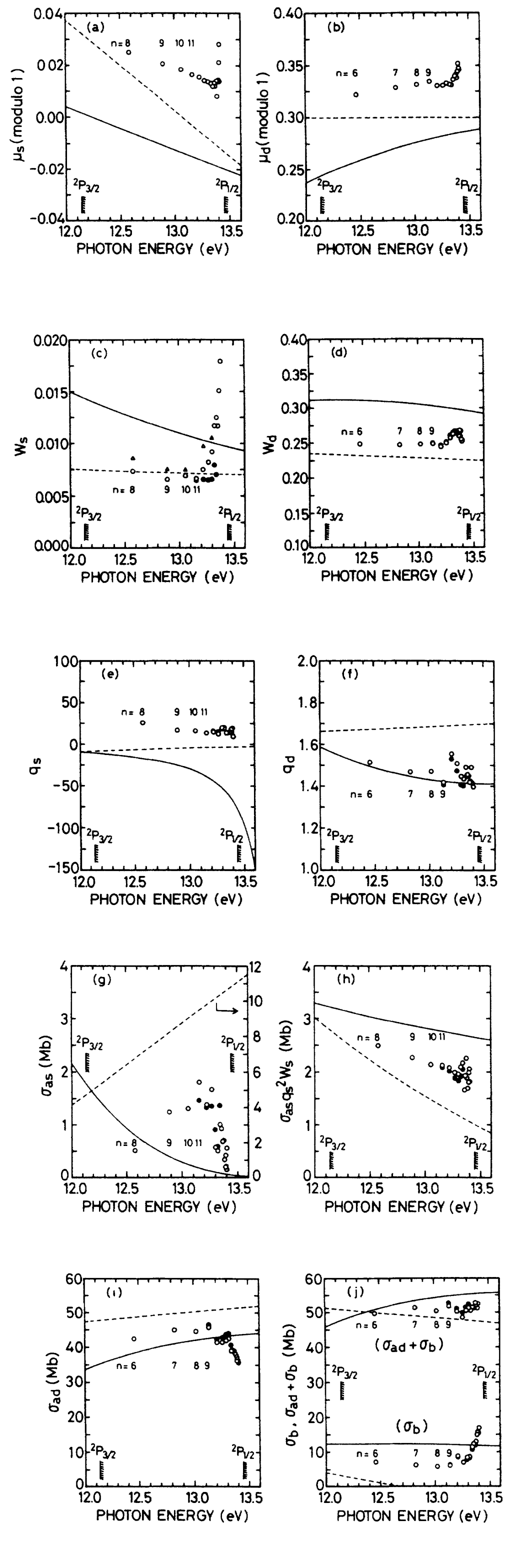

FIG. 2. Line-shape parameters for the ns' and nd' Beutler-Fano resonances of Xe. ○, present measurement in which the finite instrumental resolution is not accounted; ●, present measurement in which corrections are made for the Gaussian instrumental function (7.4 mÅ FWHM); △, measured by Wu *et al.* [10]; dashed curve, calculated from semiempirical MQDT parameters by Geiger [13]; solid curve, calculated from *ab initio* RRPA-MQDT [14] parameters provided by Cheng [22].

crease in the original W_s is therefore attributed to the lack of instrumental resolution in dealing with the width of the ns' resonances with $n > 11$. Bonin, McIlrath, and Yoshino [4] measured the $11s'$ resonance width to be 2.57 ± 0.31 cm^{-1}. According to Eq. (4), this value corresponds to $W_s=0.063$, which is in excellent agreement with our corrected value of $W_s=0.064$ for $11s'$. Figure 2(c) includes the W_s values (△) calculated with the aid of Eq. (4) using the resonance width measured by Wu *et al.* [10]. Although they took into account the instrumental effect in an approximate manner for obtaining the linewidth, their W_s increases rapidly with an increase in energy, implying that their resolution was insufficient for obtaining the reliable linewidth.

The effect of the finite instrumental resolution can also be seen on σ_{as} in Fig. 2(g). The decrease in σ_{ad} in Fig. 2(i) and the corresponding increase in σ_b in Fig. 2(j) for high-n members might be some artifacts which could not be sufficiently compensated for at present. The other parameters μ_s, μ_d, W_d, q_s, and q_d are insensitive to the instrumental resolution. (Note that μ_l and q_l would be strictly independent of the instrumental width if the instrumental profile were Lorentzian.) The quantities $\sigma_{as}q_s^2W_s$ and $\sigma_{ad}+\sigma_b$, which correspond to the transition probabilities (per unit energy) to the s' closed channel and to the d open channel, respectively, in the absence of the s-d coupling, are also insensitive to the instrumental resolution as can be seen in Figs. 2(h) and 2(j).

IV. DISCUSSION

To compare the measured Beutler-Fano line shapes with those calculated by means of semiempirical [13] and *ab initio* [14] methods, we reproduced the photoabsorption cross sections from the semiempirical [13] and *ab initio* [14,22] MQDT parameters at certain energies and then carried out curve fitting to the calculated cross sections using Eqs. (1) and (2). The semiempirical and *ab initio* line-shape parameters thus obtained were interpolated to give the dashed and solid curves, respectively, in Fig. 2. We find general fair agreement between the measured and calculated line-shape parameters. However, we should point out some significant discrepancies between them.

As can be seen in Figs. 2(a) and 2(b), the semiempirical calculation for μ_s and μ_d show some discrepancies with the measured values. These discrepancies may be ascribed in part to the insufficient energy-level data which Geiger employed in his semiempirical MQDT analysis. It may be worthwhile to carry out the semiempirical MQDT analysis again for the updated energy-level data. However, it is beyond the scope of this paper. The *ab initio* calculation gives systematically smaller values for μ_s and μ_d and larger values for W_s and W_d than the measured ones, as can be seen in Figs. 2(a)–2(d). Wu *et al.* [10] also pointed out that the $8s'$ resonance width was overestimated by the *ab initio* calculation.

As can be seen in Fig. 2(g), the *ab initio* calculation predicts that σ_{as}, which corresponds to the transition probability to the s open channel, has a Cooper minimum just above the $I_{1/2}$ limit. Accordingly, q_s, which has a negative value in the autoionization region, decreases rapidly with an increase in energy: the extrapolation of q_s goes to $-\infty$ at the Cooper minimum. [See the solid curve in Fig. 2(e).] The measured σ_{as}, however, increases with an increase in energy, implying that σ_{as} has the Cooper minimum below the $I_{3/2}$ limit. [See Fig. 2(g).] Accordingly, the measured q_s has a positive value and decreases slowly with an increase in energy between $I_{3/2}$ and $I_{1/2}$, as can be seen in Fig. 2(e). The σ_{as} is considerably overestimated by the semiempirical calculation, as can be seen in Fig. 2(g).

The measured $\sigma_{as}q_s^2W_s$ decreases slowly with an increase in energy, as predicted by both calculations, and lies just between these two calculations. [See Fig. 2(h).] The measured σ_{ad} and $\sigma_{ad}+\sigma_b$ are in reasonable agreement with both calculations as can be seen in Figs. 2(i) and 2(j), whereas the σ_b is overestimated by the *ab initio* calculation and underestimated by the semiempirical calculation as can be seen in Fig. 2(j). (The semiempirical σ_b goes to a negative value at high energy, suggesting inappropriate extrapolation.)

In conclusion, working in the high-resolution measurement for the absolute photoabsorption cross sections in the autoionization region of Xe, we have obtained Beutler-Fano line-shape parameters as a function of photon energy, demonstrating that the high-resolution line-shape measurement provides a sensitive test of the MQDT parameters.

ACKNOWLEDGMENTS

We are grateful to Dr. K. T. Chang (Lawrence Livermore Laboratory) for providing comprehensive sets of RRPA-MQDT parameters which are not available in the literature. We are also indebted to the staff of the Photon Factory for their help. This work has been carried out under the approval of the Photon Factory Program Advisory Committee (Proposal No. 88-102).

[1] H. Beutler, Z. Phys. **93**, 177 (1935).
[2] U. Fano, Nuovo Cimento **12**, 154 (1935).
[3] K. Yoshino and D. E. Freeman, J. Opt. Soc. Am. B **2**, 1268 (1985).
[4] K. D. Bonin, T. J. McIlrath, and K. Yoshino, J. Opt. Soc. Am. B **2**, 1275 (1985).
[5] L. G. Wang and R. D. Knight, Phys. Rev. A **34**, 3902 (1986).
[6] R. E. Huffman, Y. Tanaka, and J. C. Larrabee, J. Chem. Phys. **39**, 902 (1963).
[7] P. H. Metzger and G. R. Cook, J. Opt. Soc. Am. **55**, 516 (1965).
[8] F. M. Matsunaga, R. S. Jackson, and K. Watanabe, J. Quantum Spectrosc. Radiat. Transfer **5**, 329 (1965).
[9] J. H. Eland, cited by J. Berkowitz, *Photoabsorption, Photoionization, and Photoelectron Spectroscopy* (Academic, New York, 1979), p. 181.
[10] J. Z. Wu, S. B. Whitfield, C. D. Caldwell, M. O. Krause, P. van der Meulen, and A. Fahlman, Phys. Rev. A **42**, 1350 (1990).
[11] M. J. Seaton, Rep. Prog. Phys. **46**, 167 (1983).
[12] K. T. Lu, Phys. Rev. A **4**, 579 (1971); C.-M. Lee and K. T. Lu, Phys. Rev. A **8**, 1241 (1973).
[13] J. Geiger, Z. Phys. A **282**, 129 (1977).
[14] W. R. Johnson, K. T. Cheng, K.-N. Huang, and M. Le Dourneuf, Phys. Rev. A **22**, 989 (1980).
[15] J. P. Connerade, J. Phys. B **16**, L329 (1983); Comments At. Mol. Phys. **17**, 199 (1986).
[16] J. Dubau and M. J. Seaton, J. Phys. B **17**, 381 (1984).
[17] K. Ueda, Phys. Rev. A **35**, 2484 (1987); J. Opt. Soc. Am. B **4**, 424 (1987).
[18] U. Fano and J. W. Cooper, Phys. Rev. **137**, A1364 (1965).
[19] K. Ueda, K. Maeda, K. Ito, and T. Namioka, J. Phys. B **22**, L481 (1989).
[20] K. Maeda, K. Ueda, K. Ito, and T. Namioka, Phys. Scr. **41**, 464 (1990).
[21] K. Ito, K. Maeda, Y. Morioka, and T. Namioka, Appl. Opt. **28**, 1813 (1989).
[22] K. T. Chen, unpublished data tables of RRPA-MQDT parameters.